PERGAMON

Polyhedron 20 (2001) 3219–3224

POLYHEDRON

www.elsevier.com/locate/poly

Structures of Pb(II) porphyrins: [5,10,15,20-*tetrakis*-triisopropylsilylethynylporphinato]lead(II) and [5,15-bis-(3,5-bis-*tert*-butylphenyl)-10,20-bis-triisopropylsilylethynylporphinato]lead(II)

M. John Plater [a],*, Stuart Aiken [a], Thomas Gelbrich [b,1], Michael B. Hursthouse [b,1], Grant Bourhill [c,2]

[a] *Department of Chemistry, University of Aberdeen, Meston Building, Room G103, Meston Walk, Aberdeen AB24 3UE, UK*
[b] *Department of Chemistry, University of Southampton, Highfield, Southampton, SO17 1BJ, UK*
[c] *Defence Science and Technology Laboratory, Great Malvern, St. Andrews Road, Worcestershire WR14 3PS, UK*

Received 3 August 2001; accepted 6 September 2001

Abstract

The crystal structures of two lead containing porphyrins are described. Structure **1** contains unprecedented stacks of three metalloporphyrins. Each structure shows disorder of the Pb atoms which are situated out of the mean plane of the porphyrin ring.

Keywords: Porphyrin; Lead(II); Optical limiter

1. Introduction

Optical limiters or reverse saturable absorbers are materials which display diminishing transmittance with increasing incident light intensity. This attenuation of the optical throughput can be used to protect various sensors against damage from pulsed laser sources [1–5]. Porphyrins and phthalocyanines are promising candidates for certain applications. Population of triplet-excited states is desirable since triplet states are longer lived than singlet states which enhances the limiters performance. Hence dyes, which contain heavy atoms, are of interest because heavy atoms can promote intersystem crossing. The two lead porphyrins reported here were prepared for these studies. The solid-state structures are of interest since concentrated solutions of certain lead porphyrins aggregate which diminishes their optical limiting performance.

2. Results and discussion

[5,10,15,20 - *Tetrakis* - triisopropylsilylethynylporphinato]lead(II), (**1**) crystallises in the monoclinic space group *Cc*. Fig. 1 displays one of the three independent molecules in the asymmetric unit. Crystallographic data and selected bond distances and angles for **1** can be found in Tables 1 and 2, respectively. Pb and the four nitrogen atoms form a distorted square pyramid with the metal atom in an apical position and the nitrogen occupying the corners of the base plane. A similar arrangement resembling the lead coordination by four oxygen atoms in PbO is described for Pb(TPrP) (TPrP = 5,10,15,20-tetra-*n*-propylporphyrin), the only other Pb(II) porphyrin that has been analysed by X-ray crystallography so far [6]. The distances between Pb and the least-squares plane through the four coordinat-

---

* Corresponding author. Tel.: +44-1224-272-943; fax: +44-1224-272-921.

E-mail addresses: m.j.plater@abdn.ac.uk (M.J. Plater), gelbrich@soton.ac.uk (T. Gelbrich), grant.bourhill@sharp.co.uk (G. Bourhill).

[1] Fax: +44-2380-596-723.

[2] Fax: +44-1865-747-719.

PII: S0277-5387(01)00932-9

ing nitrogen atoms are 1.235(4), 1.274(4) and 1.233(4) Å, respectively. The Pb–N bond distances vary between 2.388(8) and 2.449(8) Å and fall into the range observed for Pb(TPrP) [6]. The two different types of N–Pb–N bond angles have values between 116.3(3) and 118.6(3)° and between 73.2(3) and 75.1(3)°, respectively. The diagonal N···N separation is 4.10(1)–4.13(1) Å, similar values are observed in metal-free porphyrins. Depending on the size of the metal-ion accommodated by the tetradentate ligand, metalloporphyrins with square planar metal centres show a wide variation in their mean diagonal N···N distances from 4.25 Å for Cd(II) to 3.74 Å for Ni(II), and the macrocycles with shorter separations are significantly puckered [7,8].

The structure motif of **1**, shown in Fig. 2, is a metal-over-metal stack consisting of three molecules where all porphyrin mean planes are essentially parallel. Fig. 3 shows that the three macrocycles are staggered in such a way that the sandwiched molecule is rotated with respect to the two outer molecules by approximately 45° about the Pb1···Pb2···Pb3 axis. The macrocycle is slightly distorted from planarity with bond distances and angles showing the expected values.

Each of the three independent lead atoms is disordered over two positions related by approximate *m* symmetry with the porphyrin mean plane serving as a pseudo-mirror plane. An independent refinement of the site occupancy factors resulted in almost identical parameters for the three major lead positions Pb1, Pb2 and Pb3. The only reasonable interpretation of the disorder, illustrated in Fig. 2, is that all Pb–X vectors within the same stack always point in the same direction, when X is defined as the centroid of a N_4 base plane of each square pyramid around Pb. The site occupancy for the major component set was refined to 0.88(1). Furthermore, the staggered arrangement allows the four $-C{\equiv}C-Si(Pr^i)_3$ moieties of the central molecule to fill the holes left by the $-C{\equiv}C-Si(Pr^i)_3$ fragments of its two neighbours. The shape of each stack is dominated, as a consequence, by these voluminous side chains. Hence, the van der Waals surface of a given stack is not significantly altered with the inversion of Pb–X vector which is essential for the occurrence of the described Pb disorder. The separation between adjacent Pb atoms in the same stack of 3.782(4) and 3.768(4) Å do not imply a direct metal–metal interaction, and the separations between the respective centroids X are 3.75(1) and 3.80(1) Å. Intermolecular Pb···N distances within a stack lie between 3.147(8) and 3.35(8) Å.

The described structure motif of metal-over-metal stacks of three metalloporphyrins is, to the best of our knowledge, unprecedented. Fig. 3 shows how this particular arrangement of porphyrins with four equally voluminous (5, 10, 15, 20) bonded side chains creates an effectively filled space around each macrocycle in the stack. The packing of these stacks in the crystal struc-

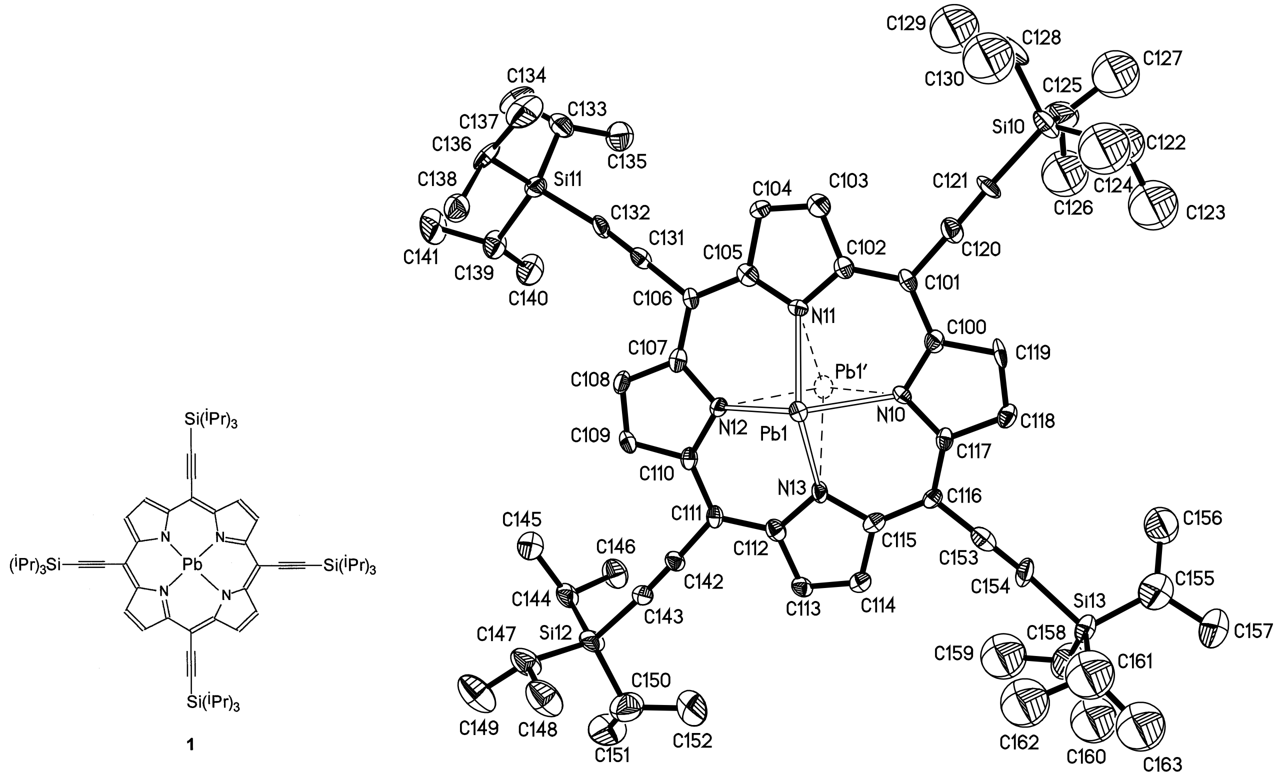

Fig. 1. Line drawing and structure of one of the three independent molecules of **1** showing 30% probability ellipsoids.

Table 1
Crystal data and structure refinement parameters for **1** and **2**

Compound	**1**	**2**
Empirical formula	$C_{192}H_{276}N_{12}Pb_3Si_{12}$	$C_{70}H_{92}N_4PbSi_2$
Formula weight	3710.90	1252.85
Crystal system	monoclinic	triclinic
Space group	Cc	$P\bar{1}$
Unit cell dimensions		
a (Å)	39.4327(6)	13.2543(4)
b (Å)	19.1701(3)	15.0949(5)
c (Å)	26.5605(4)	19.0357(7)
α (°)		72.367(1)
β (°)	104.519(1)	85.210(1)
γ (°)		64.666(1)
V (Å^3)	19436.7(5)	3275.8(2)
Z	4	2
Crystal	dark-green block	colourless block
Crystal size (mm)	$0.20\times0.15\times0.10$	$0.12\times0.10\times0.10$
θ Range (°)	2.9–25.0	3.0–25.0
Reflections collected	47 857	23 825
Independent reflections/R_{int}	24 895/0.086	11 392/0.063
Data completeness (%)	99.7	98.2
Data/parameters	24 895/1872	11 392/760
R_1/wR_2 [$F^2>2\sigma(F^2)$]	0.059/0.121	0.054/0.109
R_1/wR_2 (all data)	0.099/0.133	0.081/0.116
Absolute structure parameter	0.037(5)	
Goodness-of-fit on F^2	0.967	1.045
Largest difference peak and hole (e Å^{-3})	1.43 and −0.79	1.30 and −1.56

Table 2
Selected bond lengths (Å) and angles (°) for **1**

Bond lengths			
Pb1–N12	2.388(8)	Pb2–N23	2.419(8)
Pb1–N10	2.391(8)	Pb2–N22	2.449(8)
Pb1–N11	2.410(8)	Pb3–N32	2.384(8)
Pb1–N13	2.413(8)	Pb3–N31	2.390(8)
Pb2–N20	2.407(8)	Pb3–N33	2.400(8)
Pb2–N21	2.411(8)	Pb3–N30	2.404(8)
Bond angles			
N12–Pb1–N10	118.6(3)	N20–Pb2–N22	116.3(3)
N12–Pb1–N11	73.9(3)	N21–Pb2–N22	74.1(3)
N10–Pb1–N11	75.7(3)	N23–Pb2–N22	74.1(3)
N12–Pb1–N13	74.8(3)	N32–Pb3–N33	74.3(3)
N10–Pb1–N13	74.2(3)	N31–Pb3–N33	117.4(3)
N11–Pb1–N13	117.6(3)	N32–Pb3–N30	118.6(3)
N20–Pb2–N21	74.3(3)	N31–Pb3–N30	75.1(3)
N20–Pb2–N23	73.2(3)	N33–Pb3–N30	74.3(3)
N21–Pb2–N23	116.7(3)	N32–Pb3–N31	74.8(3)

ture is presented in Fig. 4. This arrangement is not repeated in the structure of **2** where two of the side chains are 3,5-bis-*tert*-butylphenyl groups that have a shape somewhat different from that of –C≡C–Si(Pr^i)$_3$. Infinite metal-over-metal columnar ABAB stacks are known to be formed by partially oxidised metalloporphyrins [9–11]. In these structures the infinite stacks are surrounded by anions, in most cases I_3^- chains. It is not entirely clear what prevents the formation of infinite stacks in **1**, and both the facts that the metal centre is not square planar and the bulkiness of the –C≡C–Si(Pr^i)$_3$ groups could be the contributing factors.

5,15-Bis-(3,5-bis-*tert*-butylphenyl)-10,20-bis-triisopropylsilylethynylporphyrin (**2**) crystallises in the triclinic space group $P\bar{1}$ with $Z=2$. Fig. 5 shows the molecular structure of **2**. Crystallographic data and selected bond distances and angles for **2** can be found in Tables 1 and 3, respectively. Similar to **1**, the Pb coordination by four nitrogen atoms is square-pyramidal, and the distance between Pb and the centroid of the base plane is 1.182(2) Å.

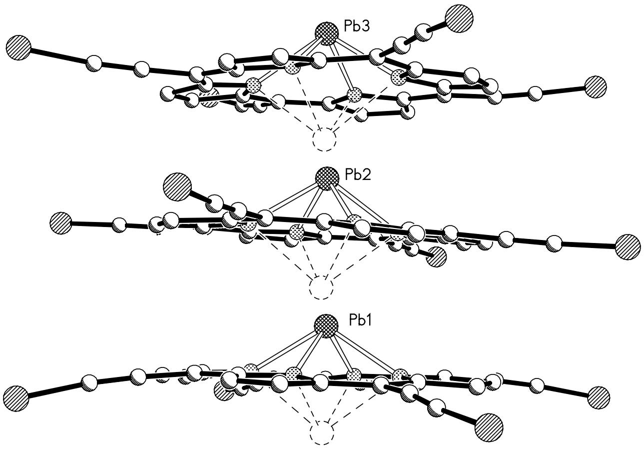

Fig. 2. Stack of three molecules in **1**. *i*-Pr groups have been omitted for clarity.

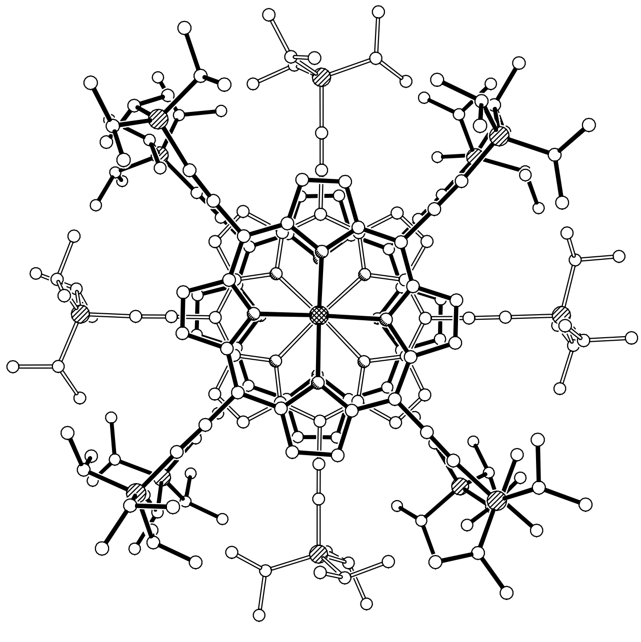

Fig. 3. Staggered arrangement of three molecules forming one single stack of **1**.

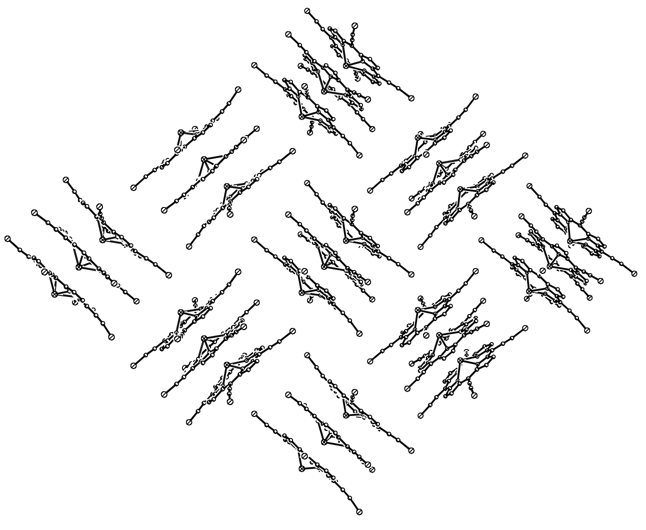

Fig. 4. Packing arrangement of stacks in the crystal structure of **1**. *i*-Pr groups have been omitted for clarity.

The core of the molecule of **2** shows the same basic features as discussed for **1**, though with a wider variation in Pb–N bond lengths, 2.332(4)–2.411(5) Å. The diagonal N–Pb–N angles are slightly increased to values between 120.7(2) and 119.7(2)°, and the other N–Pb–N angles lie between 75.1(2) and 76.0(2)°. This structure exhibits a disorder of the Pb atom similar to that described for **1** with the final site occupancy factor for the major component being 0.90(1). In the neighbouring molecule this Pb disorder is accompanied by a disorder of one of the isopropyl groups (C62 > C64) attached to Si2. Fig. 6 shows the packing arrangement of **2** which is fundamentally different from that of **1**. Each of the –C≡C–Si(Pr^i)$_3$ fragments is sandwiched by the macrocycles of two neighbouring molecules in such a way that the three –C≡C–Si– fragments involved arrange themselves in an antiparallel fashion.

Table 3
Selected bond lengths (Å) and bond angles (°) for **2**

Bond lengths			
Pb1–N4	2.332(4)	Pb1–N3	2.383(4)
Pb1–N1	2.362(4)	Pb1–N2	2.411(5)
Bond angles			
N4–Pb1–N1	75.8(2)	N4–Pb1–N2	119.7(2)
N4–Pb1–N3	75.1(2)	N1–Pb1–N2	75.5(2)
N1–Pb1–N3	120.7(2)	N3–Pb1–N2	76.0(2)

3. Experimental

Ultraviolet spectra were recorded in a Perkin–Elmer Lambda 15 UV–Vis spectrophotometer using $CHCl_3$ as the solvent. Infrared spectra were recorded in an ATI Mattson FTIR spectrometer. ^1H and ^{13}C NMR spectra were obtained at 250 and 62.9 MHz, respectively, in a Brucker AC 250 spectrometer. Chemical shifts, δ, are

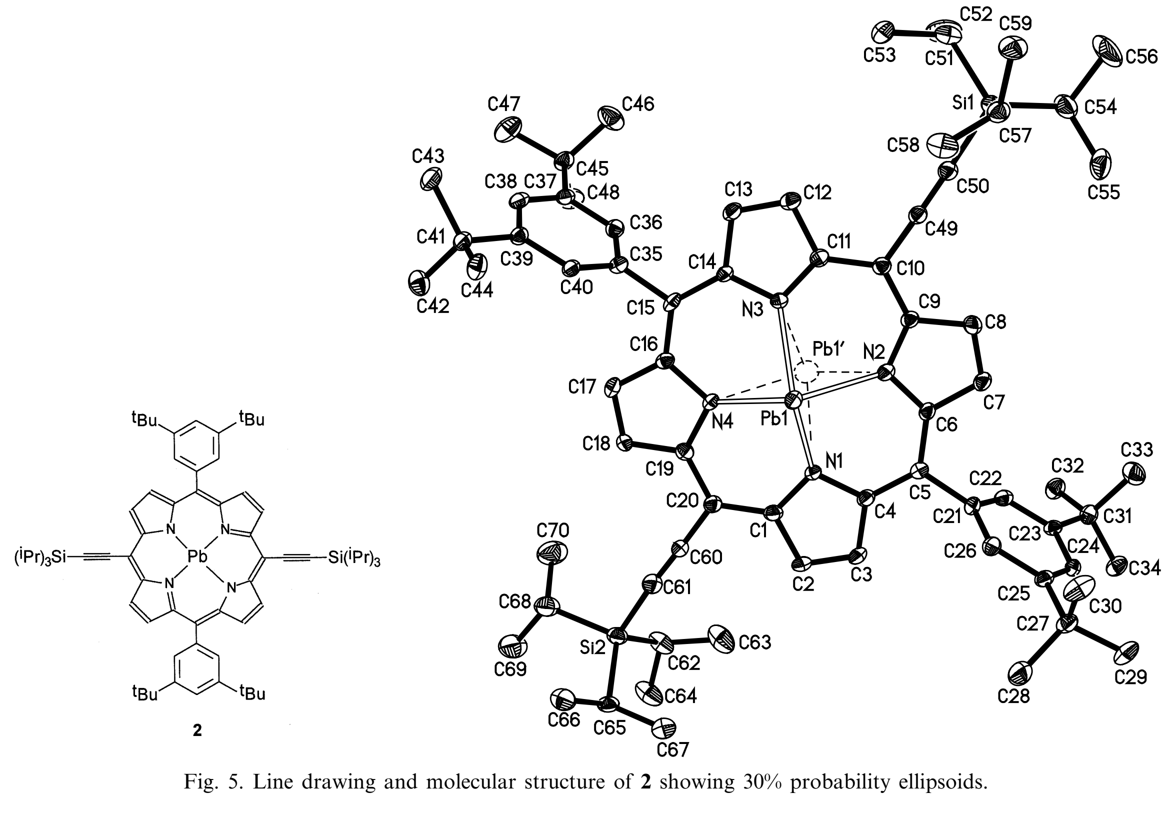

2

Fig. 5. Line drawing and molecular structure of **2** showing 30% probability ellipsoids.

given in parts per million relative to the residual solvent. Coupling constants, *J*, are given in hertz. Low-resolution mass spectra were obtained using electrospray ionisation in a Finnigan Navigator Mass Spectrometer and accurate mass at the University of Wales, Swansea using fast atom bombardment methods. Elemental analyses were obtained from Butterworth Laboratories using a PE 2400 CHN analyser. Melting points were carried out using a Kofler hot-stage microscope and are uncorrected.

3.1. *X-ray structure determinations*

Details of the crystal data and a summary of data collection parameters are given in Table 1. Intensity data for **1** and **2** were recorded at 150 and 120 K, respectively, using a Nonius Kappa CCD area-detector diffractometer mounted at the window of a rotating anode FR591 generator with a molybdenum anode (0.71073 Å). ϕ and ω scans (2° increments) were carried out to fill the Ewald sphere. Data collection and processing were carried out using the programs DIRAX, COLLECT, DENZO and MAXUS, and an empirical absorption correction was applied using SORTAV [12–16]. The structure was solved by direct methods and refined on F^2 by full-matrix least-squares refinements [17,18]. In both structures all hydrogen atoms were included in the refinement in calculated positions using a riding model.

3.2. *5,10,15,20-Tetrakis-triisopropylsilyl-ethynylporphyrin*

Boron trifluoride etherate (1.1 ml) was added to a stirred solution of pyrrole (3.80 g, 10 mmol) and 3-tri-isopropylsilylpropargylaldehyde (11.95 g, 10 mmol) in DCM (5 l) cooled to -78 °C. The solution was allowed to warm to room temperature (r.t.) over 2 h. Stirring was continued for a further 1 h, DDQ (9.7 g, 7.5 mmol) was added, stirring continued for 10 min and the solution filtered through silica. The solvent was removed under reduced pressure and the residue, dissolved in light petroleum–DCM (1:1), filtered through silica. The solvent was removed under reduced pressure and the residue was crystallised from DCM–MeOH to give the *title compound* (3.96 g, 27%) as a purple solid with metallic lustre, melting point (m.p.) >250 °C; Found: C, 74.7; H, 9.1; N, 5.6. $C_{64}H_{94}N_4Si_4$ requires C, 74.5; H, 9.2; N, 5.4%; λ_{max} ($CHCl_3$, nm): 450 ($\log \varepsilon = 5.7$), 607 (4.9) and 710 (4.3); ν_{max} (KBr, cm^{-1}): 457m, 572m, 669s, 705vs, 794m, 877m, 914w, 987m, 1058w, 1132m, 1238m, 1342w, 1459s, 1502w, 1616w, 2136s, 2356w, 2858s, 2942s, 3407m, 3478m and 3544m; δ_H (250 MHz; $CDCl_3$) -1.76 (2H, s, N–H), 1.44 and 1.46 (84H, 2 × s, *i*-Pr), 9.55 (8H, s, β-pyrrolic); δ_C (62.9 MHz; $CDCl_3$) 11.9, 19.1, 100.3, 102.6 and 107.7 (two resonances are missing); *m*/*z* 1031.8 (M^+, 100%).

3.3. *[5,10,15,20-Tetrakis-triisopropylsilylethynyl-porphinato]lead(II)* (**1**)

A mixture of 5,10,15,20-*tetrakis*-triisopropylsilyl-ethynylporphyrin (0.71 g, 0.5 mmol) and $Pb(OAc)_2 \cdot 3H_2O$ (2 g, 5 mmol) in DMF (60 ml) was heated at reflux. After 2 h water was added and the precipitate filtered, washed with water, MeOH and recrystallised from DCM–MeOH to give the *title compound* (0.54 g, 90%) as a green solid, m.p. >250 °C; Found: C, 62.0; H, 7.4; N, 4.4. $C_{64}H_{92}N_4Si_4Pb$ requires C, 62.1; H, 7.5; N, 4.5%; λ_{max} ($CHCl_3$, nm): 500 ($\log \varepsilon = 5.8$) and 719 (4.9); ν_{max} (KBr, cm^{-1}): 457m, 516w, 572m, 665s, 709vs, 788m, 877m, 993m, 1058m, 1149s, 1203m, 1238w, 1315w, 1380w, 1463s, 2130s, 2858s, 2935s, 3408m, 3476m and 3547w; δ_H (250 MHz; $CDCl_3$) 1.50 and 1.51 (84H, 2 × s, *i*-Pr) and 9.67 (8H, s, β-pyrrolic); δ_C (62.9 MHz; $CDCl_3$) 12.0, 19.3, 99.3,

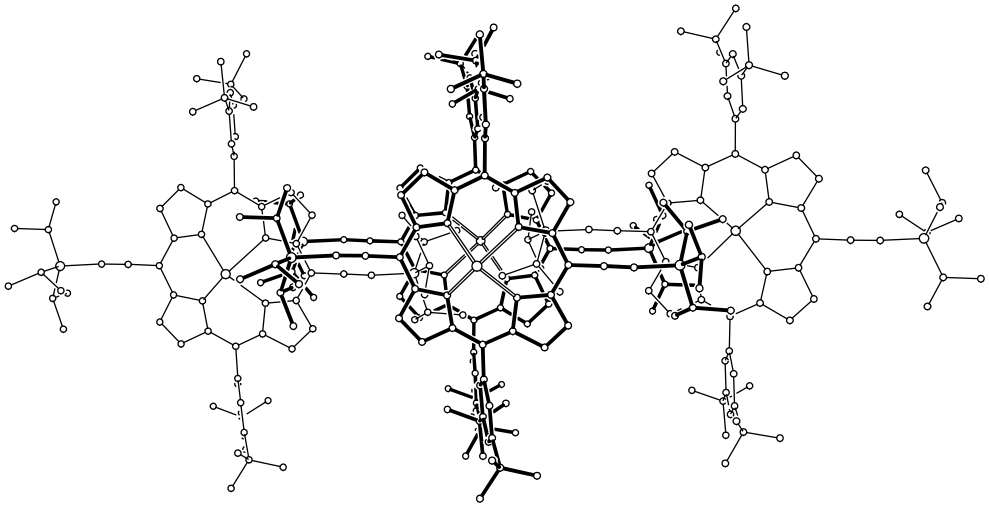

Fig. 6. Packing arrangement of four molecules in the crystal structure of **2**.

104.1, 108.7, 131.9 and 151.2; *m*/*z* 1236 ($M^+ + H$, 100%).

3.4. 5,15-Bis-(3,5-bis-tert-butylphenyl)-10,20-bis-triisopropylsilylethynylporphyrin

Under argon, $BF_3 \cdot Et_2O$ (0.1 ml) was added to a stirred solution of *meso*-(3,5-di-*tert*-butylphenyl)-2,2′-dipyrrylmethane (753 mg, 2.2 mmol) and 3-triisopropylsilylpropargylaldehyde (500 mg, 2.4 mmol) in DCM (1 l) and the solution stirred. After 1 min, DDQ (0.768 g, 3.4 mmol) was added and stirring continued for 20 min more. The solution was filtered through silica, the solvent removed under reduced pressure and the residue chromatographed on silica with light petroleum–dichloromethane (1:1) as eluent. The second fraction was collected and the solvent removed under reduced pressure to give the *title compound* (230 mg, 20%) as a purple crystalline solid, m.p. > 300 °C (dichloromethane–methanol). Larger preparations of this compound can be purified by repeated crystallisation. Found: C, 79.2; H, 9.0; N, 5.0. $C_{70}H_{94}N_4Si_2 \cdot CH_3OH$ requires C, 79.0; H, 9.15; N, 5.2%; λ_{max} ($CHCl_3$, nm): 434 ($\log \varepsilon = 5.7$) and 585 (4.9); ν_{max} (KBr, cm^{-1}): 2959vs, 2862s, 2139m, 1591m, 1558w, 1473m, 1427w, 1363m, 1263w, 1245m, 1136m, 1069m, 985m, 915m, 881m, 801s, 715s, 676m and 580w; δ_H (250 MHz; $CDCl_3$) −2.11 (s, 2H, N–H), 1.42 (42H, m, *i*-Pr), 1.53 (36H, s, *t*-Bu), 7.80 (2H, t, $J = 1.8$ Hz, *p*-Ph), 8.01 (4H, d, $J = 1.8$ Hz, *o*-Ph), 8.86 (4H, d, $J = 4.6$ Hz) and 9.64 (4H, d, $J = 4.6$ Hz); δ_C (62.9 MHz; $CDCl_3$) 11.9, 19.1, 31.8, 35.1, 99.1, 100.9, 108.8, 121.4, 123.1, 129.4, 130.4, 131.9, 140.4 and 148.9 (two resonances are missing); *m*/*z* 1047 (M^+, 100%).

3.5. [5,15-Bis-(3,5-bis-tert-butylphenyl)-10,20-bis-triisopropylsilylethynylporphinato]lead(II) (2)

A suspension of 5,15-bis-(3,5-bis-*tert*-butylphenyl)-10,20-bis-triisopropylsilylethynylporphyrin (40 mg, 0.04 mmol) and $Pb(OAc)_2 \cdot 3H_2O$ (1.2 g, 3 mmol) in DMF (20 ml) was refluxed for 4 h under argon. The resulting deep green solution was poured into water (50 ml). The precipitate was filtered, washed with water, MeOH and recrystallised from DCM–MeOH to give the *title compound* (30 mg, 63%) as a deep green, almost black, solid, m.p. > 300 °C (dichloromethane–methanol). Found: C, 67.9; H, 7.5; N, 4.35. $C_{70}H_{92}N_4PbSi_2$ requires C, 67.1; H, 7.4; N, 4.5%; λ_{max} ($CHCl_3$, nm): 473 ($\log \varepsilon$ 5.3), 493 (5.3) and 704 (4.6); ν_{max} (KBr, cm^{-1}): 2955vs, 2862s, 2361w, 2332w, 2134m, 1589m, 1470m, 1389w, 1361m, 1280m, 1244m, 1207s, 1157m, 1062w, 995m, 923m, 880m, 794m, 717vs, 670m and 565w; δ_H (400 MHz; $CDCl_3$) 1.55 (78H, m, *t*-Bu and *i*-Pr), 7.82 (2H, t, $J = 2$ Hz, *p*-Ph), 7.87 (2H, bs, *o*-Ph), 8.19 (2H, bs, *o*-Ph), 8.99 (4H, d, $J = 4$ Hz) and 9.78 (4H, d, $J = 4$ Hz); δ_C (100.6 MHz; $CDCl_3$) 13.0, 20.2, 32.8, 36.0, 99.5, 103.4, 110.7, 122.2, 126.6, 131.0, 132.0, 134.2, 142.3, 150.3 and 152.5 (one resonance is missing); *m*/*z* 1252.6623 (M^+ $C_{70}H_{92}N_4Si_2Pb$ requires 1252.6627), 1252.7 (M^+, 100%).

4. Supplementary material

Crystallographic data for the structural analysis have been deposited with the Cambridge Crystallographic Data Centre, CCDC Nos. 167552 and 167553 for compounds **1** and **2**, respectively. Copies of this information may be obtained free of charge from The Director, CCDC, 12 Union Road, Cambridge, CB2 1EZ, UK (fax: +44-1223-336033; e-mail: deposit@ccdc.cam.ac.uk or www: http://www.ccdc.cam.ac.uk).

References

[1] R. Crane, K. Lewis, E. van Stryland, M. Khoshnevisan (Eds.), Materials for optical limiting, Proceedings of the MRS, 1996, p. 374.

[2] K. Mansour, D. Alvarez, K.J. Perry, I. Choong, S.R. Marder, J.W. Perry, Proc. SPIE 1853 (1993) 132.

[3] K. Mansour, P. Fuqua, S.R. Marder, B. Dunn, J.W. Perry, Proc. SPIE 2143 (1994) 239.

[4] (a) J.W. Perry, K. Mansour, S.R. Marder, C.-T. Chen, P. Miles, M.E. Kenney, G. Kwag, Proc. MRS 374 (1996) 257;
(b) P. Le Barny, V. Dentan, P. Robin, F. Soyer, M. Vergnolle, SPIE 2852 (1996) 201.

[5] P.V. Bedworth, J.W. Perry, S.R. Marder, Chem. Commun. (1997) 1353.

[6] K.M. Barkigia, J. Fajer, A.D. Adler, G.J.B. Williams, Inorg. Chem. 19 (1980) 2057.

[7] M.O. Senge, M.W. Renner, W.W. Kalisch, J. Fajer, J. Chem. Soc., Dalton Trans. (2000) 381.

[8] M.P. Byrn, C.J. Curtis, I. Goldberg, Yu Hsiou, S.I. Khan, P.A. Sawin, S.K. Tendick, C.E. Strouse, J. Am. Chem. Soc. 113 (1991) 6549.

[9] L.J. Pace, J. Martinsen, A. Ulman, B.M. Hoffman, J.A. Ibers, J. Am. Chem. Soc. 105 (1983) 2612.

[10] T.P. Newcomb, M.R. Godfrey, B.M. Hoffman, J.A. Ibers, Inorg. Chem. 29 (1990) 223.

[11] K. Liou, T.P. Newcomb, M.D. Heagy, J.A. Thompson, W.B. Heuer, R.L. Musselman, C.S. Jacobsen, B.M. Hoffman, J.A. Ibers, Inorg. Chem. 31 (1992) 4517.

[12] A.M. Duisenberg, J. Appl. Crystallogr. 25 (1992) 92 (DIRAX).

[13] R. Hooft, B.V. Nonius, COLLECT: Data Collection Software, 1998.

[14] Z. Otwinowski, W. Minor, in: C.W. Carter Jr., R.M. Sweet (Eds.), Macromolecular Crystallography, Part A. In: Methods in Enzymology, vol. 276, Academic Press, New York, 1997, pp. 307–326 (DENZO).

[15] S. Mackay, C.J. Gilmore, C. Edwards, M. Tremayne, N. Stewart, K. Shankland, MAXUS: A Computer Program for the Solution and Refinement of Crystal Structures from Diffraction Data.

[16] SORTAV: (a) R.H. Blessing, Acta Crystallogr., Sect. A 51 (1995) 33;
(b) R.H. Blessing, J. Appl. Crystallogr. 30 (1997) 421.

[17] P.T. Beurskens, G. Beurskens, W.P. Bosman, R. de Gelder, S. Garcia-Granda, R.O. Gould, R. Israël, J.M.M. Smits, DIRDIF-96, Crystallography Laboratory, University of Nijmegen, The Netherlands, 1996.

[18] G.M. Sheldrick, SHELXL-97, University of Göttingen, Göttingen, Germany, 1997.